A METAL DROPLET LEVITATED IN THE AMPLITUDE-MODULATED AC MAGNETIC FIELD

B. Bardet[1], *J. Priede*[2], *J. Etay*[1]

[1] *CNRS INPG EPM-Madylam, ENSHMG BP 95 St Martin d'Hères cedex, France*
[2] *Institute of Physics, University of Latvia, 32 Miera, LV-2169, Salaspils, Latvia*

Introduction. Electromagnetic levitation method is widely used for measurements of thermophysical properties of liquid metals. For example, surface tension and viscosity can be determined from the frequency and damping rate of shape oscillations, respectively. The usual approach is to excite an initial surface deformation and then to observe relaxation of its oscillations in time. This method is rather technically complicated because it requires a direct visual observation of the shape of surface and identification of different oscillation modes. We propose a different approach based on the analysis of shape oscillations in frequency rather than time domain. The idea of the method is to force shape oscillations with various frequencies and to observe their amplitude. The oscillations are forced by supplying the levitation coil with an amplitude-modulated AC current. Variation of the droplet shape and its position in the coil affect the total inductance of the coil, which, in turn, causes variation of AC frequency of a self-tuning power generator. Thus the shape oscillations forced by amplitude modulation cause, in turn, a modulation of the AC frequency, which is used to evaluate the amplitude oscillations. The resonance frequencies in the measured spectra are related to the surface tension, whereas the width of resonance peaks is related to the viscosity of the melt. In this work we simply compare model and experimental results related to static levitation only: free surfaces, inductance variation and frequency of horizontal oscillations of a solid sphere. We find that an axisymmetric model yields a good agreement with experiment.

1. Experimental set-up.

1.1. The test cell. The experimental facility for electromagnetic levitation, built at the EPM-Madylam laboratory, comprises 3 parts: a cell of experiment, an electrotechnical part, and a recording system. The test section (Fig. 1*a*) is a cell made from a quartz tube of 140 mm in diameter and closed by two caps. The bottom cap, made of electrically insulating material, contains both the through passes for electrical connections of the inductor and a mobile stem for putting of the solid load into the inductor (Fig. 1*b*). The top cap, made of steel, incorporates a vacuum tube, argon supply, and a through pass for a contact probe or a thermocouple. The electrotechnical equipment includes a high-frequency generator made by CELES that powers an oscillatory circuit consisting of an inductor and a set of capacitors. The inductor comprises 4 basic and 2 counter-windings similarly to the numerical model of Bojarevics Ref. [1]. The control and acquisition system is described in Ref. [2]. The load used for levitation was nickel.

1.2. Image processing. A standard 25 Hz video camera was used to record the droplet. A mirror was placed at 45° so that two perpendicular views of the droplet on each image were visible. This allowed us to observe 3D-shape of the droplet. Shape of the droplet was averaged over the time period of 2 seconds by digitalizing 50 images. From each image a contour of the droplet was extracted by choosing an average level of the blue color. The extracted contours were verified to be insensitive to the selected threshold level. The main frequencies of the vertical

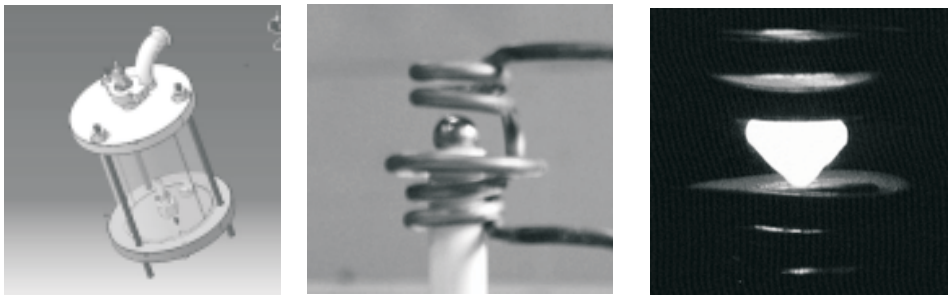

(a) (b) (c)

Fig. 1. Experimental set-up: enclosure of test – in the center the nickel sphere on its support before fusion – on the right the molten load of nickel in levitation.

and horizontal oscillations of a solid sphere were obtained from Fourier spectrum of its mass center coordinates.

2. Numerical method. The magnetic field around an axisymmetric droplet in the inductor modeled by a set thin circular current loops was calculated in the perfect-conductor approximation by a surface integral equation method in terms of the azimuthal component of the vector potential of magnetic field:
$A(\mathbf{r}) = A^e(\mathbf{r}) + A^i(\mathbf{r})$, where $A^e(\mathbf{r})$ is the external vector potential generated by the coil; $A^i(r) = 1/4\pi \int_l \partial(r'A(\mathbf{r}'))/\partial n' G(\mathbf{r},\mathbf{r}') r' \mathrm{d}l'$ is the induced vector potential; L is the contour forming surface of the axisymmetric droplet;
$G(\mathbf{r},\mathbf{r}') = 2/\sqrt{r'r}\,[(2/k - k)\,K(k) - 2/k E(k)]$ is the Green's function defined in terms of the complete elliptical integrals of the first and second kind, $K(k)$ and $E(k)$, respectively, of modulus $k = 2\sqrt{r'r/\left((r+r')^2 + (z-z')^2\right)}$. This surface integral equation has to be solved with respect to the unknown surface current distribution defined by $\partial(r'A(\mathbf{r}'))/\partial n'$ satisfying boundary condition $A(\mathbf{r})|_L = 0$ at the surface of the load assumed to be perfectly conducting here. This problem was solved numerically by using the boundary element method with constant elements. Equilibrium shape of the droplet was found by the using a variational approach requiring minimization of the total associated energy which may be written in a dimensionless form with the following gravitational, surface, and magnetic field contributions [3]:

$$U = 2\pi \left[\int_L \left(1 + \mathrm{Bo}\,|\mathbf{r}|^{\,2} \mathbf{e}_z \cdot \mathbf{n}/2\right) r \mathrm{d}l - \mathrm{Bm} \sum_n r_n I_n A^i(\mathbf{r}_n) \right],$$

where $\mathrm{Bo} = \rho g a^2/\gamma$ is the usual Bond number defined in terms of load density ρ, surface tension γ, load radius a, and free fall acceleration g; $\mathrm{Bm} = \mu_0 I_0^2/(4\gamma a)$ is the magnetic Bond number containing in addition the current amplitude I_0, and permeability of vacuum μ_0. The last sum in the expression above is taken over the loops constituting the coil and represents the energy of the magnetic field associated with the currents induced in the load. Note that this expression excludes the self-energy of the coil which is formally divergent for a thin-winding model but, however, independent of the induced currents.

3. Results.

3.1. Droplet shapes. Fig. 2 shows comparison of droplet shapes observed experimentally with those calculated numerically. The shapes were recorded within two seconds after melting of the droplet in order to minimize the effects of variation of the thermophysical properties with the temperature. In Fig. 2, the filled

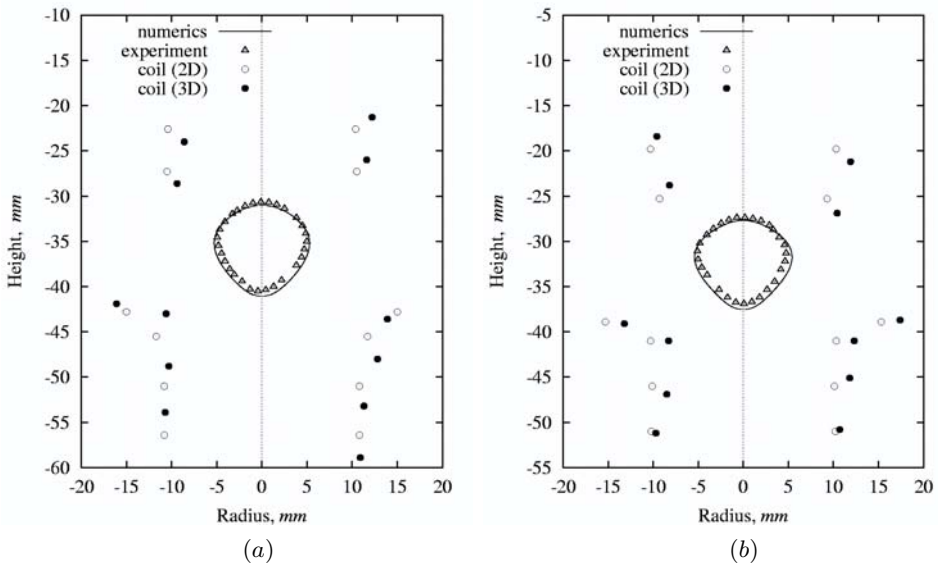

Fig. 2. Front (*a*) and side (*b*) views of experimentally observed shapes of a droplet of 10 mm in characteristic diameter together with the corresponding numerical results for $I_{\text{eff}} = 428$ A effective current at $f = 274\,200$ Hz AC frequency; • – cross-section positions of the real 3D inductor; ∘ – averaged positions of an axisymmetric inductor used for numerical simulation.

circles mark cross-section centers of the coil tube, whereas hollow circles mark the averaged positions of the corresponding axisymmetric coil used for numerical simulations. The comparison is done for the load of 10 *mm* in characteristic diameter at the effective current $I_{\text{eff}} = 428$ A with the AC frequency $f = 274\,200$ Hz. As seen, both the calculated shape and position of the droplet are close to the experimental observations. It is interesting to note that the difference between the numerical and experimental shapes slightly differs depending on the view. Thus, for front view the shape difference defined as the average of the distance between the closest pairs of experimental and numerical surface points is equal to 13% to and 15% for the front and side views shown in Figs. 2*a* and 2*b*, respectively. The difference of the vertical positions of the centre of mass of the calculated and measured drop is 1.08 mm. These discrepancies can be attributed to the very rough approximation used for calculations. Better agreement with experiment is obtained when the real size and shape of the inductor tube is taken into account. Additional significant discrepancy between the experiment and calculation is due to the zero skin depth approximation applicable for shielding parameters greater than 300, while in experiment the shielding parameter was only about 80. In the present case, the calculated power in the load is underestimated leading to a calculated position lower than the experimental one.

3.2. Comparison on the oscillation. The characteristic frequencies of mass center oscillations of solid load measured in experiment were about 8 Hz and 11.25 Hz for radial and axial directions, respectively. For the given coil design and fixed size of the load the frequencies, which are calculated according to the approach described in [4], depend in principle on both the current in the coil and the shielding parameter determined by the AC frequency. However, the numerical results evidence that the frequency practically depends on the vertical position of the load in the coil which, in turn, is determined by both the current in the coil and the shielding parameter. Direct dependence of the frequency on the shielding parameter at a fixed vertical position is weak. The vertical equilibrium positions of

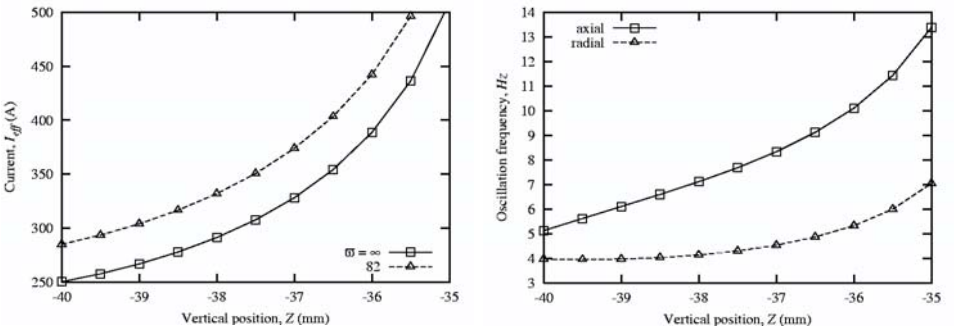

(*a*) (*b*)

Fig. 3. Efficient current versus the vertical position of Ni load of 10 mm in diameter for the AC frequency $f = 297$ kHz corresponding to shielding parameter $\varpi = 82$ in comparison to the perfect-conductor approximation corresponding to $\varpi = \infty$ (*a*). The frequency of the axial and radial mass centre oscillations of the load depending on its vertical position in the coil (*b*).

the load of characteristic diameter 10 mm are plotted in Fig. 3*a* versus the effective current at various shielding parameters. For the effective current 428 A at the AC frequency 297 kHz the axial equilibrium position is about $z = -36$ mm that, according to the frequencies plotted in Fig. 3*b*, corresponds 5.1 Hz and 9.6 Hz for the radial and axial oscillations, respectively. Note that the calculated oscillation frequencies, especially the radial one, differ noticeably from the experimentally observed ones. Nevertheless, the ratio of the calculated radial and axial frequencies is close to 2 that agrees well with the theoretical prediction for the load close to the neutral point of the magnetic field [5].

4. Conclusions. An experimental set-up has been used to test a numerical code. The effects of the inductor helicity on the shape of the load have been quantified. Results from both calculation and experiment are in good agreement. Next efforts will be related to the description of the nonstationary free surface of the sphere under a pulsating magnetic field.

Acknowledgement. This work was partly supported by ESA in the framework of the MAP-Thermolab project. JP is grateful for the support from French-Latvian bilateral cooperation programme in science "Osmose."

REFERENCES

1. V. Bojarevics and K. Pericleous. Modelling electromagnetically levitated liquid droplet. *ISIJ Int.*, vol. 43 (2003), no. 6, pp. 890–898.
2. D. Perrier, J.P. Paulin, B. Bardet, R. Gerner, Y. Fautrelle, and J. Etay. A new way of diagnostic of the state of the load in an induction system. In *Proceedings of the 4th International Conference on Electromagnetic Processing of Materials – ISIJ Int.* (Lyon, France, 14-17 October 2003), paper C5–8.3.
3. A.D. Sneyd and H.K. Moffatt. Fluid dynamical aspects of the levitation-melting process.
4. J. Priede and G. Gerbeth. Stability of electromagnetically levitated spherical sample in a set of coaxial circular loops. *IEEE Trans. Magn.* (in press).
5. D.L. Cummings and D.A. Blackburn Oscillations of magnetically levitated aspherical droplet. *J. Fluid Mech.*, vol. 224 (1991), pp. 395–416.